Chapter 4

Results and discussion

4.1 Starting Powders

4.1.1 Ca : P ratios and Impurities of starting powders

Table 7 shows Ca:P ratios and amount of impurities, characterized by Department of Science and Services and, Mineral Assay and Services, respectively. Ca:P ratios of both MP and TP were 1.63, fewer than which the stoichiometric value, 1.67. It was indicated that MP and TP were calcium deficient hydroxyapatite (amorphous calcium phosphate,ACP). Amount of impurities in TP was less than that of MP except iron content. This might result from chemical treated process such as impurity content in the reagents.

characteristic	starting powder	
	MP	TP
Ca:P mol ratio	1.63:1	1.63:1
Impurities,		
Mg(%)	0.56	0.39
Fe(ppm)	10	220
Zn	140	20
Cu	10	10
Mn	30	40
Heavy metals, ppm		
Cd	< 4	< 4
Pb	70	40
Hg	< 0.3	< 0.3

Table 7. Ca:P ratios and impurities in starting powders.

4.1.2 Phases Present of Starting Powders

XRD pattern of MP powder, shown in Fig.40, with the highest peak at 2θ= 31.8, agreed with the powder diffraction card* of hydroxyapatite. No second phase was presented. Broader peaks of TP powder indicated its particle size which readily smaller than that of MP.

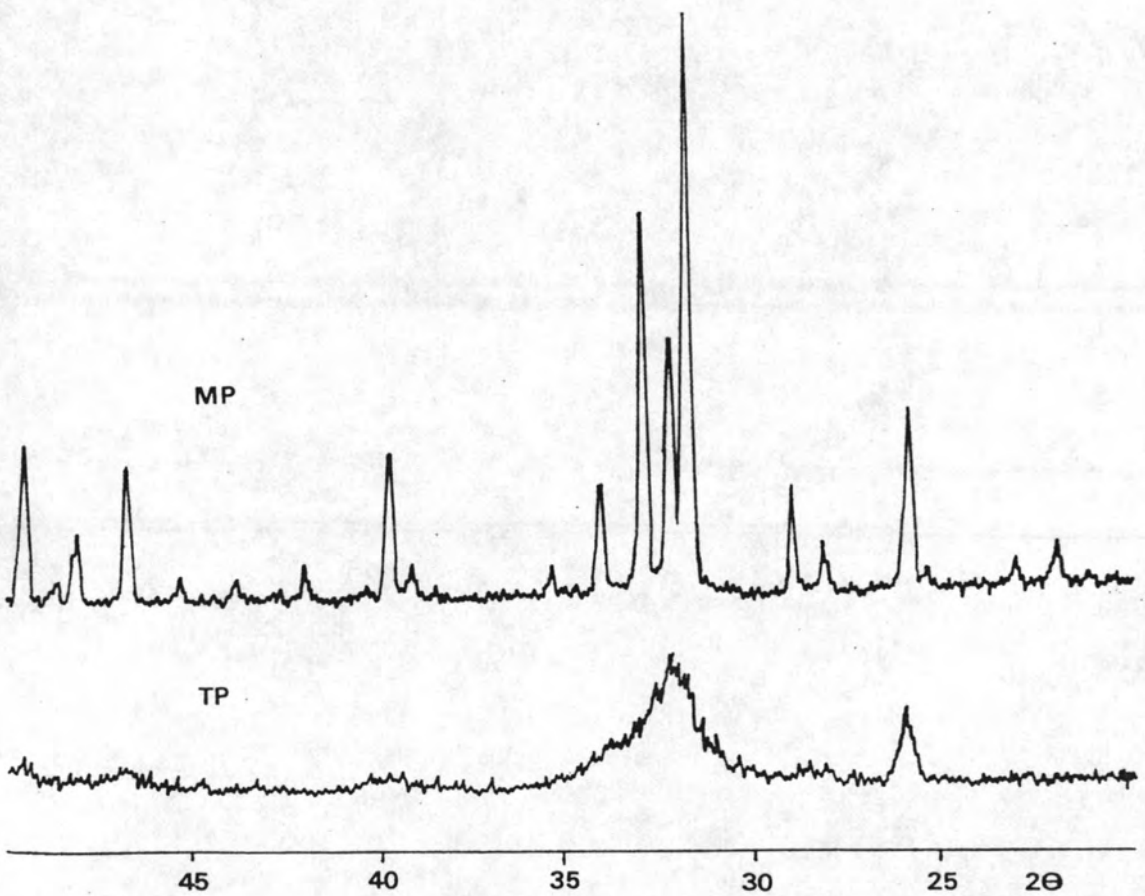

Figure 40. XRD patterns of MP and TP powders.

* see appendix A

4.1.3 Microstructure and Particle Size Distribution of Starting Powders

Microstructure of MP and TP powders derived from powder preparation step, was shown in Fig.41 and 42.

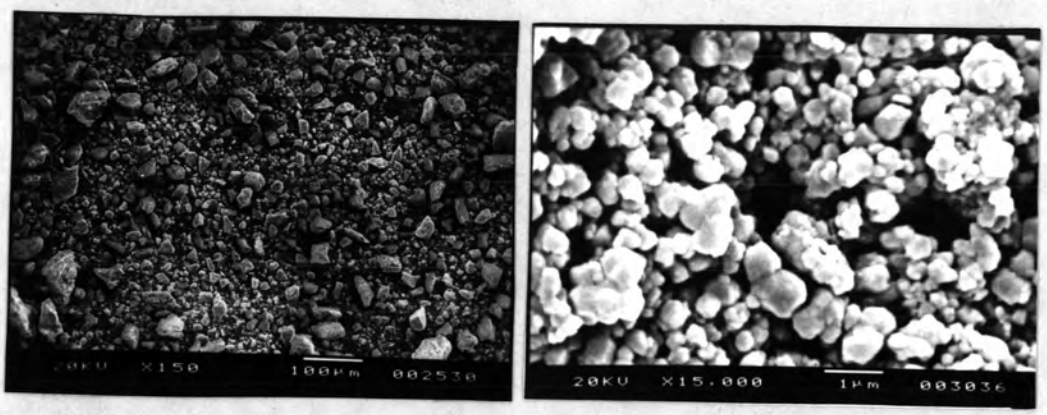

a b

Figure 41. Microstructure of MP powder.

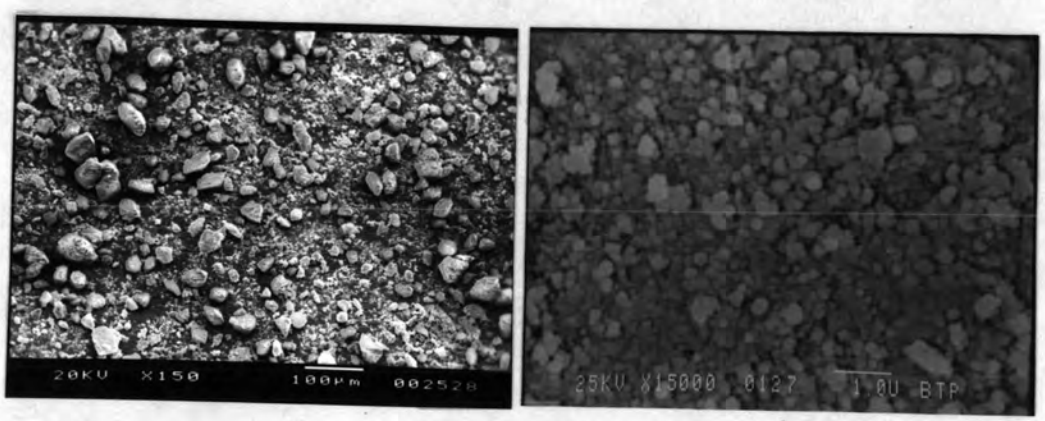

a b

Figure 42. Microstructure of TP powder.

a) agglomerates

b) primary particles

Fig.41a and 42a showed agglomerates of each powder, which contain irregular shape and various sizes. It could be roughly determined that agglomerates of MP were slighly larger than agglomerates of TP. Primary particles of these two powders were shown in fig.41b and 42b. Primary particles of MP were clearly larger than that of TP. Both MP and TP primary particles were rather of symmetrical shape.

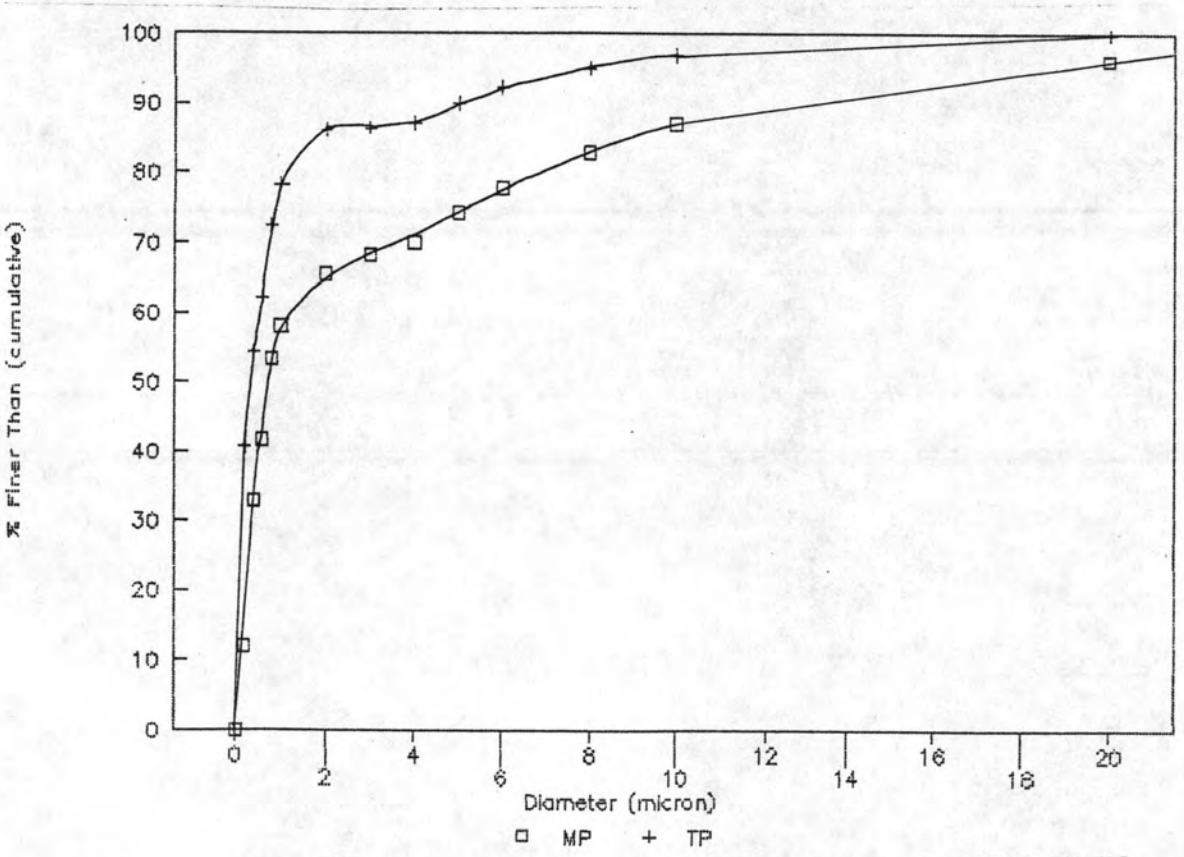

Fig 43. Particle size distribution of MP and TP powders.

Particle size distribution of MP and TP powder, determined by particle size analyzer was shown in Fig.43. From the graph, 100% of MP and TP were finer than 35 and 20 μm, respectively.When compared with the size of particles indicated from Fig.41 and 42, the sizes of particles from the graph were larger than primary particles, but smaller than agglomerates, which shown in SEM photographs. It could be concluded that particle size determined from analyzer was mixed size of primary particles and agglomerates, depends on the degree of dispersion of powder in reference solution.

4.2 Granules

Characteristics and properties of MP and TP granules derived from granulation step were shown in table 8. % Moisture content in both MP and TP granules was in the range of 8-14 %, agreed with the common granule derived from granulation described by Reed(1989). This moisture content might influenced the other properties that flow rate, filled density and tap density of TP granules were slightly lower than those of MP granules. Accordingly,the ratio of tap density to filled density which showed the packing efficiency of granules, of TP was also slighly worse than that of MP.

characteristic	granule	
	MP	TP
% PVA (by wt.)	1.60	1.60
% H_2O	10.90	11.05
aging time (days)	3	3
flow rate (g/sec)	0.49	0.42
filled density (g/cm^3)	1.07	0.88
tap density (g/cm^3)	1.10	0.97
$\frac{\text{tap density}}{\text{filled density}}$	1.03	1.10

Table 8. Characteristics of MP and TP granules.

4.3 Compact Bars

About 93 % of 650 compact bars formed by hydraulic pressing, were usable. The remaining ~7 % compact bars could not be used because of the small crack present (visually detected).

The photograph of fracture surface of MP and TP compact bars, Fig.44, indicated that TP compact bar was denser than MP. Microcracks and small pores were occasionally present in TP. Because of the denser compaction, bulk density of TP was little bit higher than that of MP (Table 9).

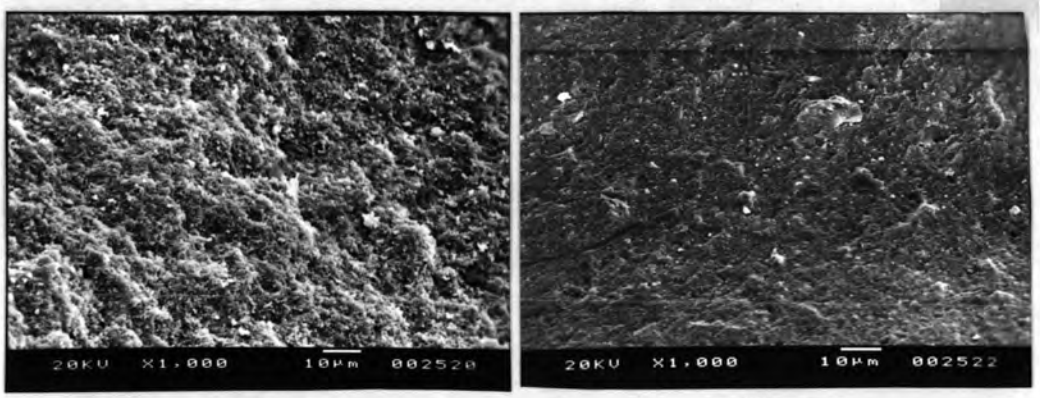

MP TP

Figure 44. Fracture surface of MP and TP compact bars.

sample	density (g/cm^3)	%theoretical density
MP	2.15	68.04
TP	2.18	68.99

Table 9. Density and %theoretical density of MP and TP bars.

4.4 Calcined Specimens

After calcination at 500 ^{o}C, grain size of MP and TP slightly increased. IT was indicated by XRD patterns where peaks of calcined particles were sharper than those of starting particles (Fig.45 compared with Fig.40). No second phase was observed in this state.

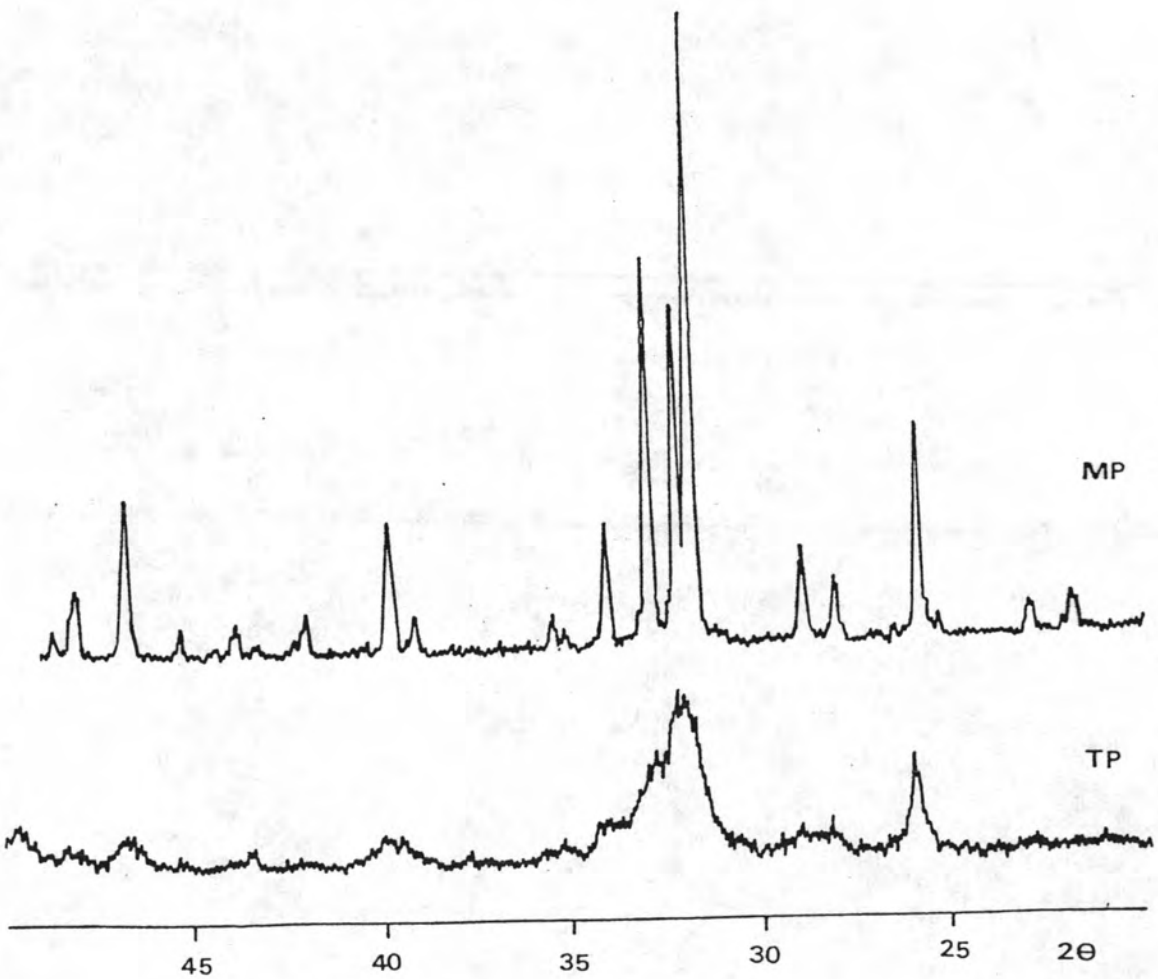

Figure 45. XRD patterns of calcined MP and TP, calcined at 500 ^{o}C.

The denser TP compaction was comfirmed again by SEM photographs (Fig.46).

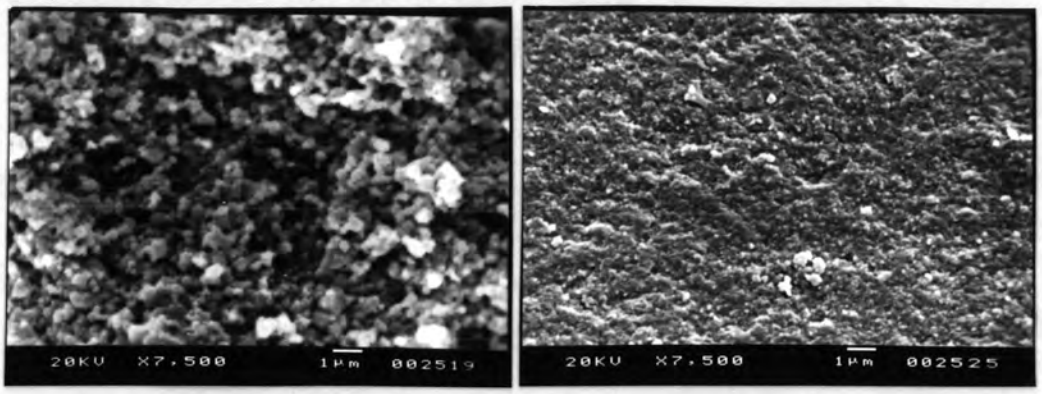

MP TP

Figure 46. Fracture surface of MP and TP calcined specimens.

The bulk density and also % theoretical density (Table 10) of TP calcined specimen were slightly higher than those of MP, similar to the result in previous step (Table 9). % Water absorption of MP calcined specimen was also slightly lower than TP.

characteristic	MP	TP
bulk density (g/cm^3)	2.21	2.27
% theoretical density	69.94	71.84
% water absorption	15.55	14.94

Table 10. Bulk density, % theoretical density and % water absorption of MP and TP calcined bars.

4.5 Coating Slips

The relation between viscosity and shear rate of MP and TP coating slips was shown in Fig. 47. It was found that the slips were thixotropic (pseudoplastic). This rheological properties were the same as other general glazes.

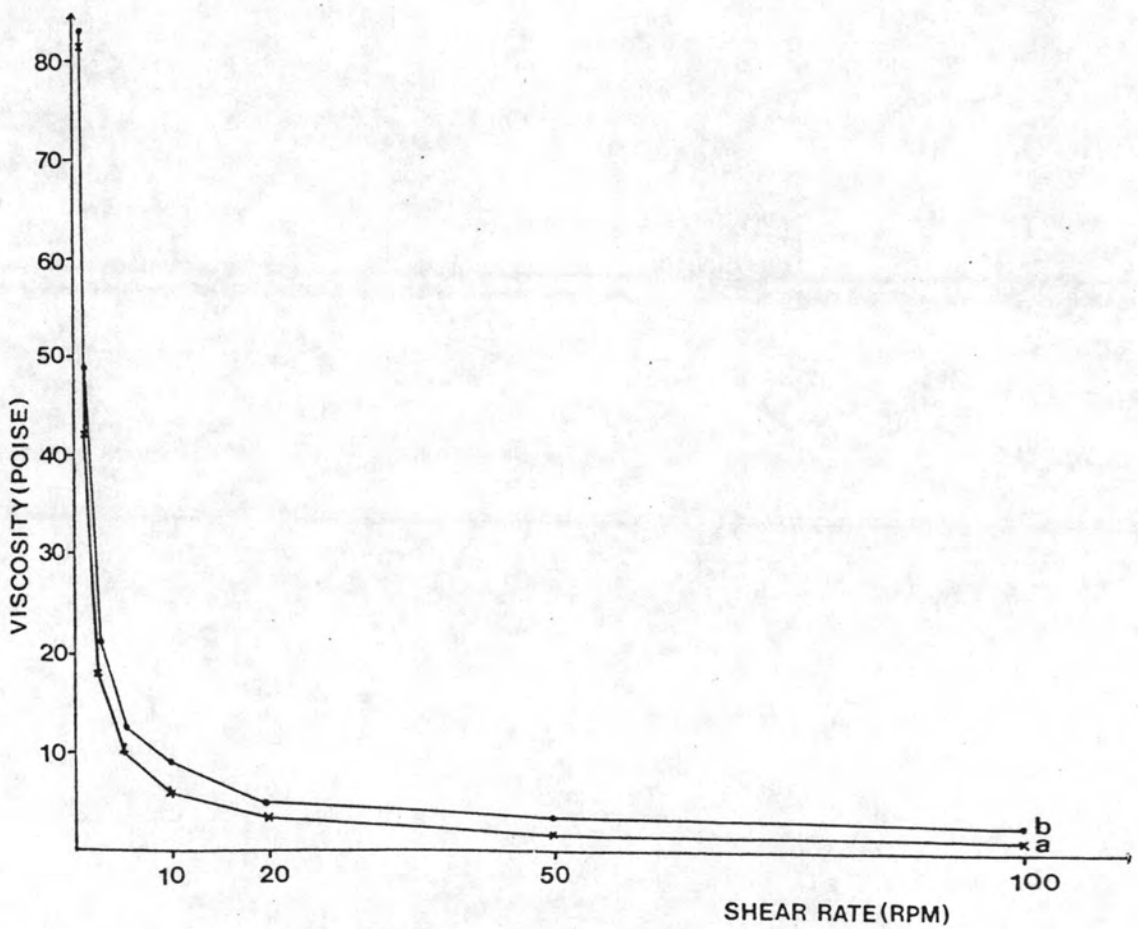

Figure 47. Rheological properties of coating slips.
a) MP coating slip
b) TP coating slip

4.6 Uncoated Products

4.6.1 Characteristics of Sintered MP and TP Bars

After sintering, ceramics usually shrink, their water absorption decreases and the bulk density increases. These are the result of pore shrinkage and grain growth during sintering process. %Water absorption, % apparent porosity, % volume shrinkage, bulk density and % theoritical density of MP and TP bars sintered at 1100, 1200 and 1300 ^{o}C were shown in Fig.48-52. As any other ceramic materials, bulk density, %theoretical density and volume shrinkage increased, and the remaining , % water absorption and % apparent porosity decreased when they were sintered at higher temperature. The bulk density of TP bars at all sintering temperatures was still higher than that of MP bars.

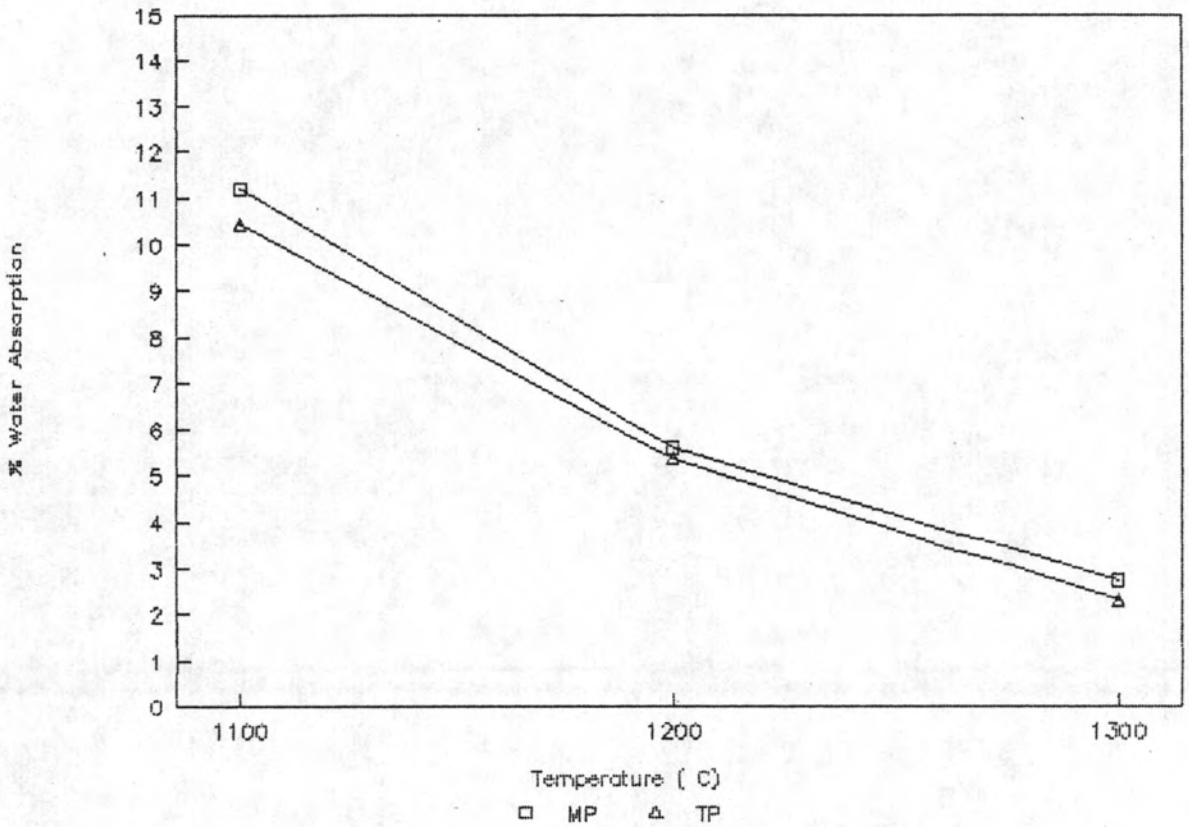

Figure 48. % Water absorption of MP and TP bars sintered at 1100, 1200 and 1300 ^{o}C.

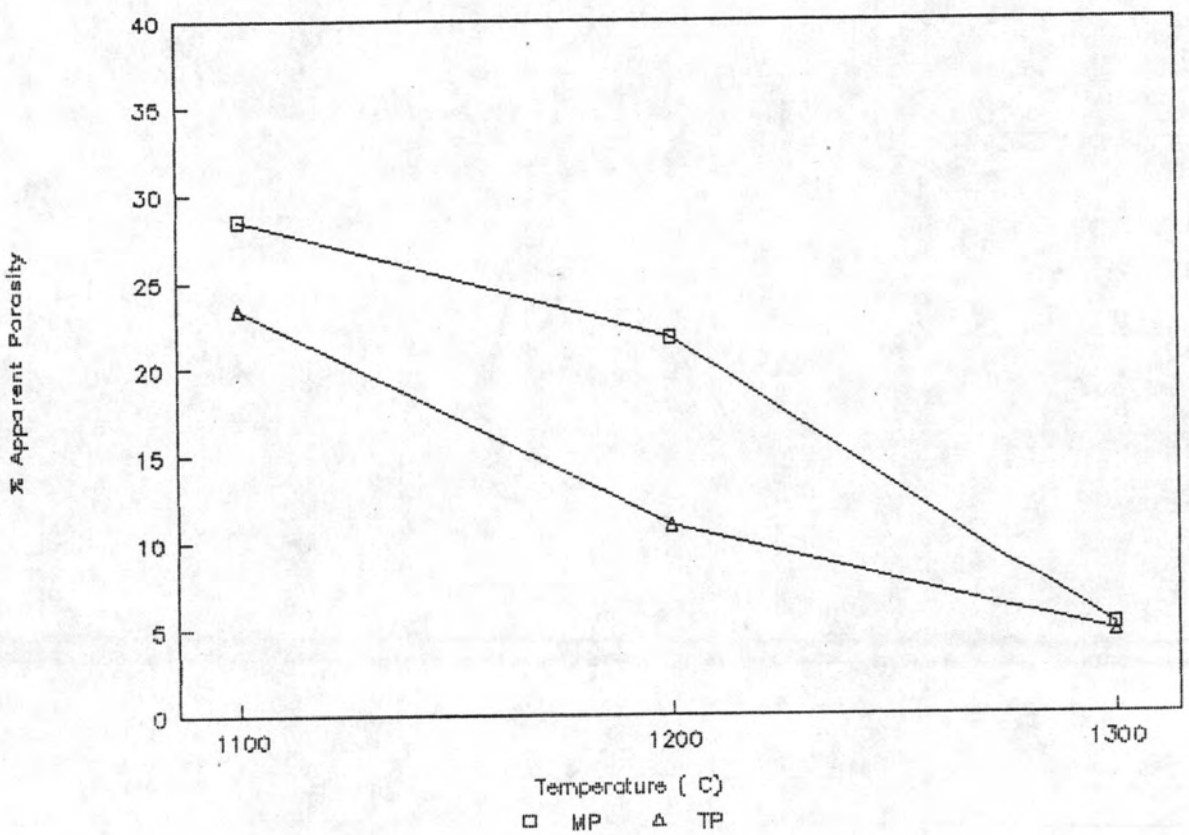

Figure 49. % Apparent porosity of MP and TP bars sintered at 1100, 1200 and 1300 ^{o}C.

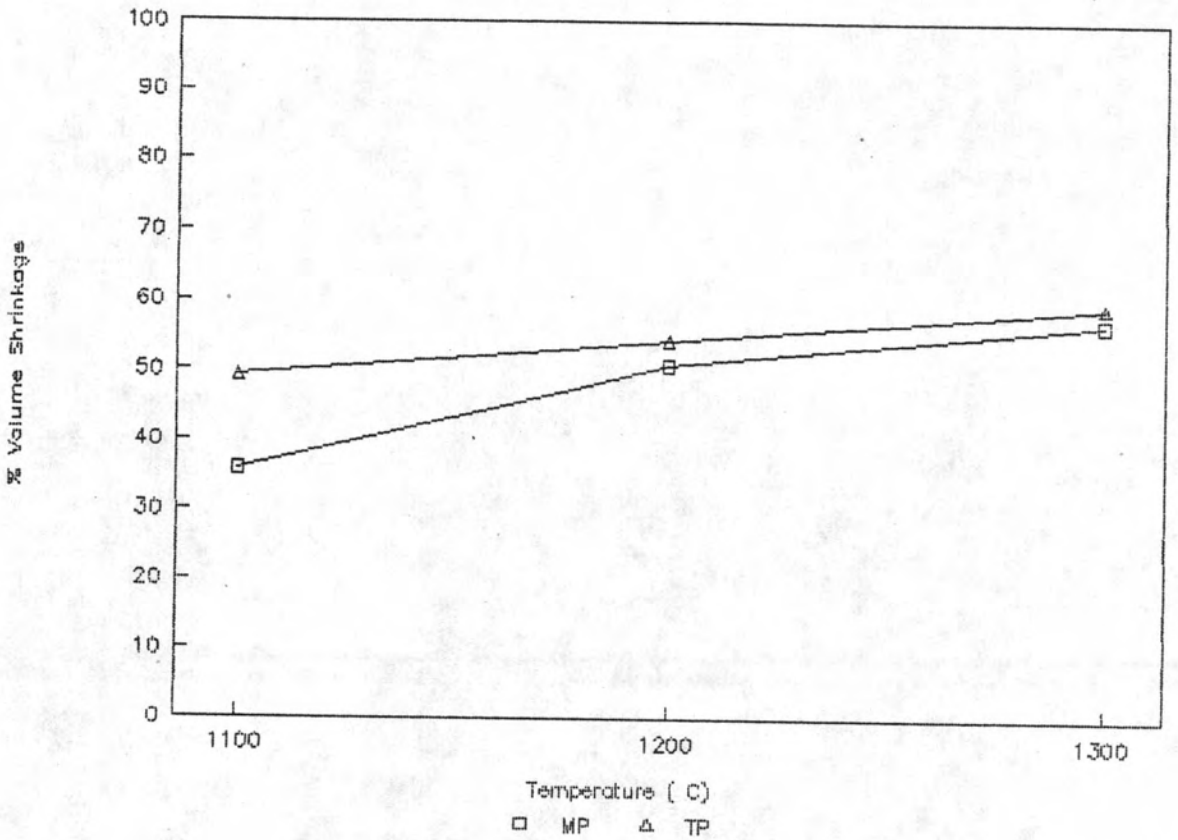

Figure 50. % Volume shrinkage of MP and TP bars sintered at 1100, 1200 and 1300 ^{o}C.

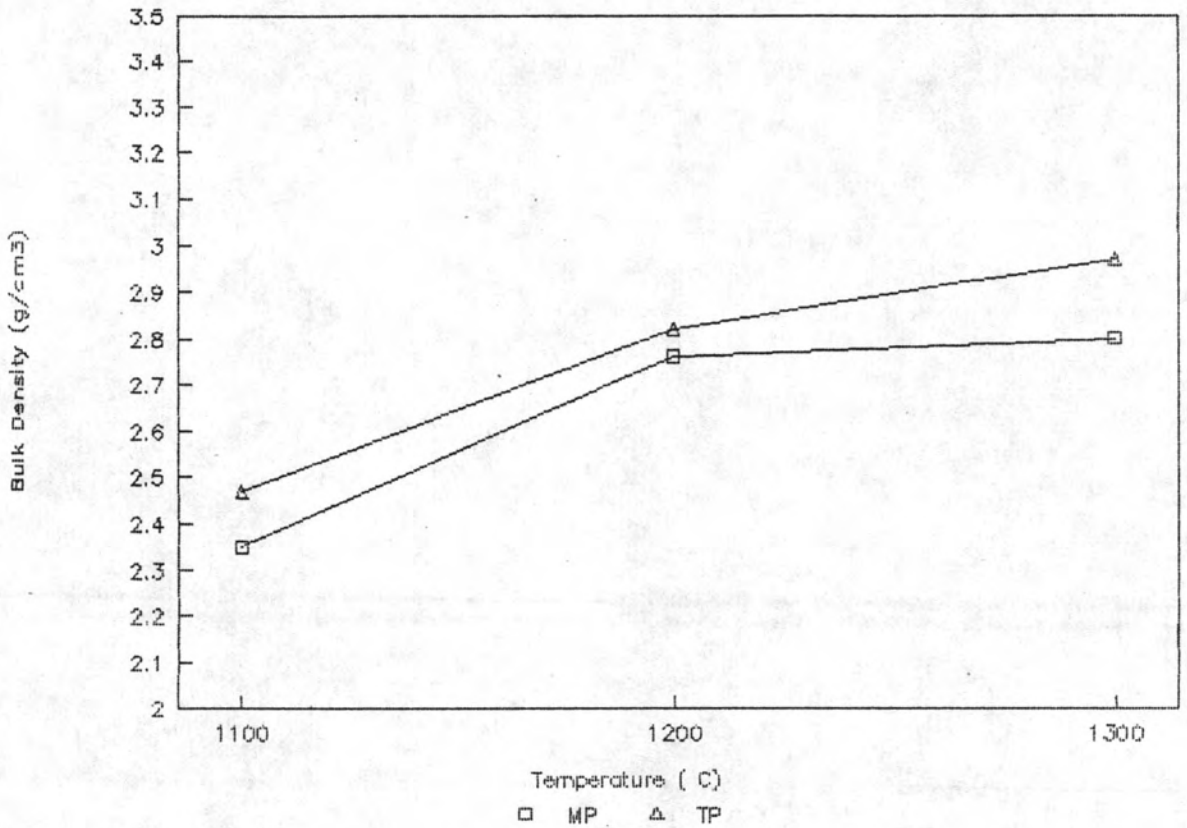

Figure 51. Bulk density of MP and TP bars sintered at 1100, 1200 and 1300 °C.

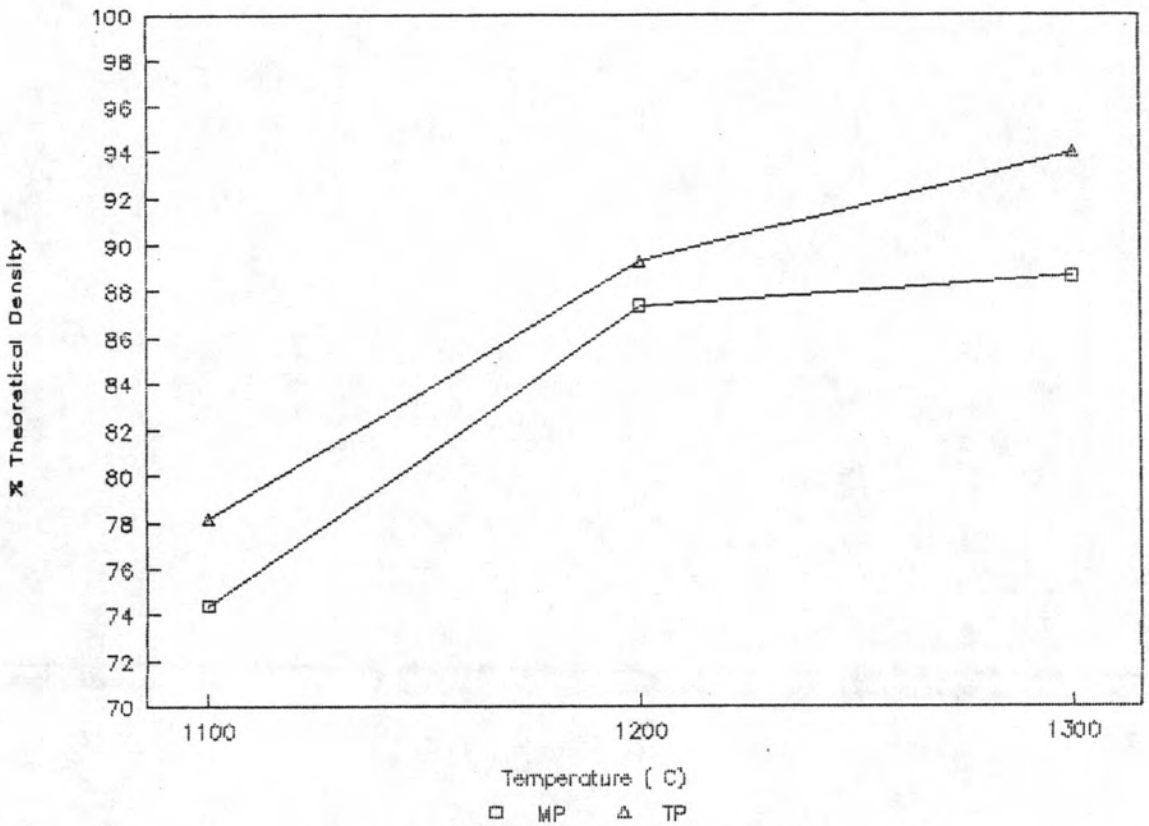

Figure 52. % Theoretical density of MP and TP bars sintered at 1100, 1200 and 1300 ^{o}C.

4.6.3 Phases Present in Sintered MP and TP

From XRD patterns(Fig.53 and 54), no second phase was detected in both MP and TP which sintered at 1100 ^{o}C. But at sintering temperature 1200 ^{o}C, there was beta tricalcium phosphate present in MP and TP. In TP, Alpha tricalcium phosphate was also present. And at sintering temperature 1300 ^{o}C, beta, alpha tricalcium phosphate and $Ca_4P_2O_9$ were detected in both MP and TP.

The occurence of all second phases was a high thermal decomposition behavior which commonly took place in non-stoichiometric hydroxyapatite as :
(Aoki, 1991)

$$Ca_{10-x}H_{2x}(PO_4)_6(OH)_2 \longrightarrow \beta\text{-}Ca_3(PO_4)_2 + Ca_{10}(PO_4)_6(OH)_2$$
$$\longrightarrow \alpha\text{-}Ca_3(PO_4)_2 + Ca_4P_2O_9$$

$$\beta\text{-}ca_3(PO_4)_2 \xrightarrow{1120\text{-}1180\ ^{o}C} \alpha\text{-}Ca_3(PO_4)_2$$

(Monma and Nagai, 1989)

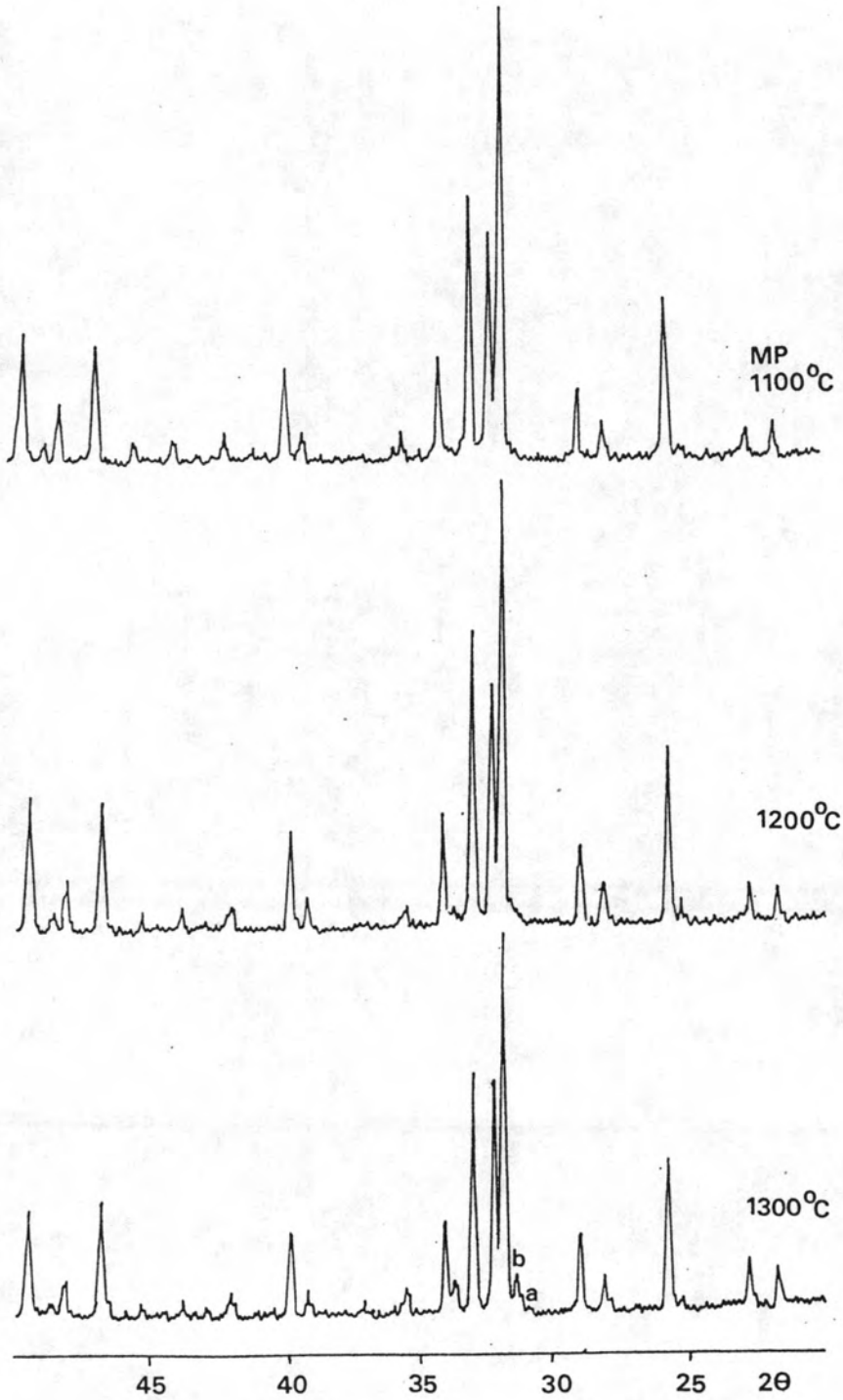

Figure 53. XRD patterns of MP sintered at 1100, 1200 and 1300 °C.

a = α-$Ca_3(PO_4)_2$

b = β-$Ca_3(PO_4)_2$

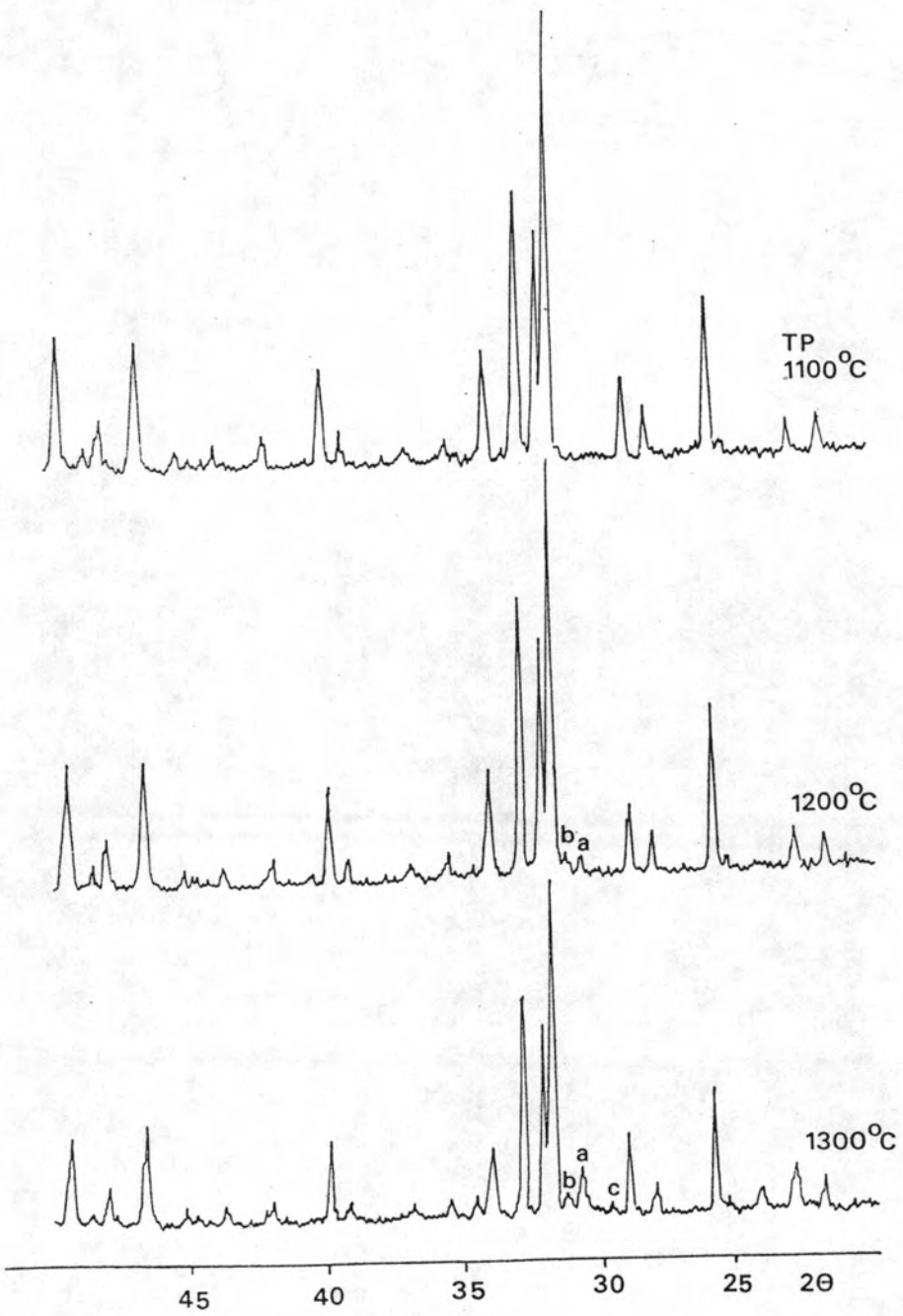

Figure 54. XRD patterns of TP sintered at 1100, 1200 and 1300 °C.

a = α-$Ca_3(PO_4)_2$

b = β-$Ca_3(PO_4)_2$

c = $Ca_4P_2O_9$

4.6.3 Microstructure of Sintered MP and TP

Fracture surfaces of sintered MP and TP bars was shown in fig.55-60. In both MP and TP, grain size increased with the increasing of sintering temperature. At the same sintering temperature, grain size of MP was still larger than that of TP.

MP TP

1100 °C

1200 °C

1300 °C

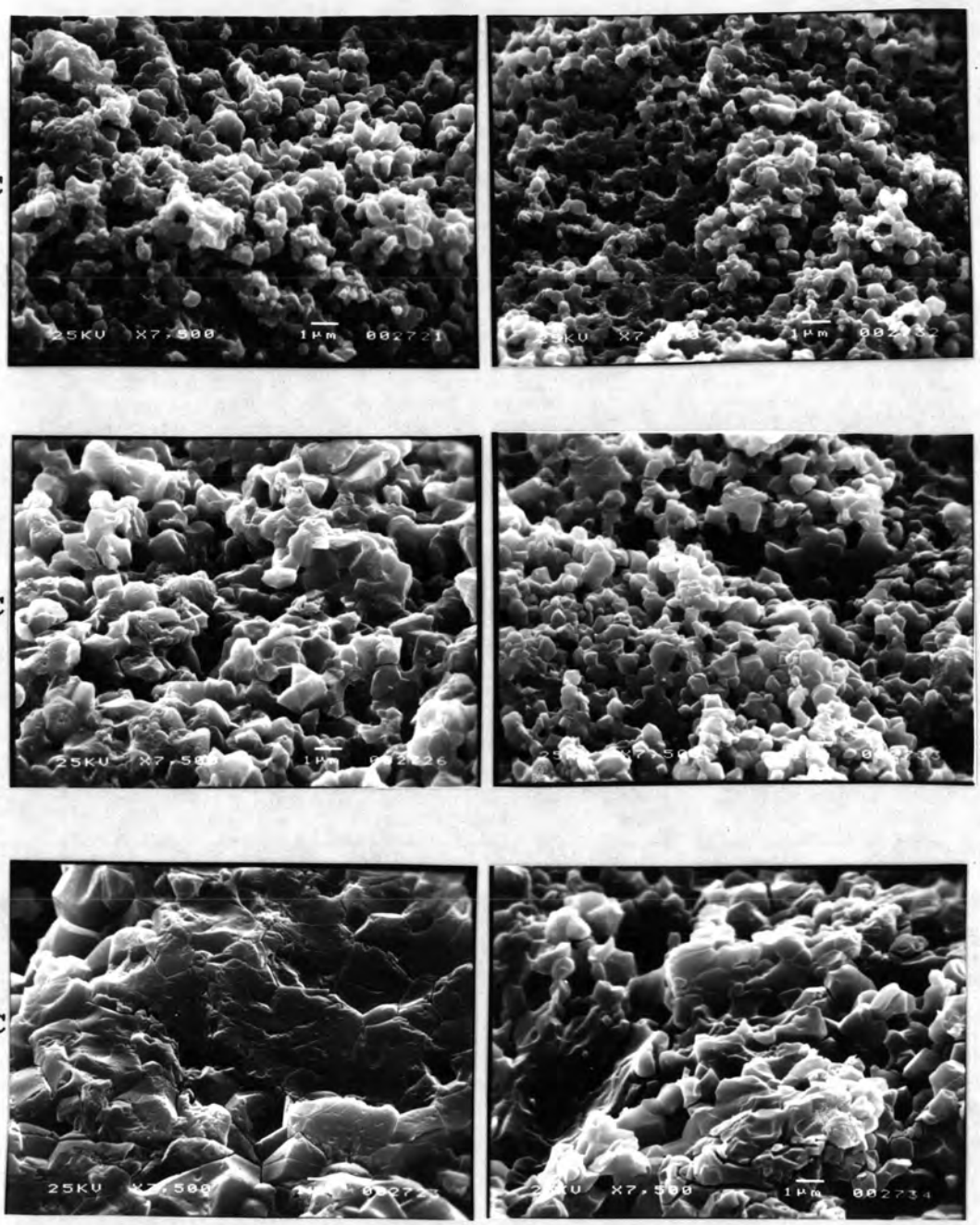

Figure 55-60. Microstructure of MP and TP bars sintered at 1100, 1200 and 1300 °C. (fracture surface)

4.7 Coated Product

4.7.1 MP bars coated with various coating composition

Cracking was visually detected in all coated MP bars. Clearly observation was carried out by the means of SEM. Surface condition of MP bars coated with various MP:TP compositions sintered at 1200 ^{o}C for 1 h was shown in Fig.61-64. More serious cracking occured when TP content in coating composition increased. This agreed with the thermal expansion result(Fig.65). From the graph,the bigger difference in thermal expansion between pure MP(MP body)and coating was indicated when the coating consisted of higher TP content. This thermal expansion difference induced the tension on the coated layer. So, the result was cracking.

MP:TP ratio

0:100

25:75

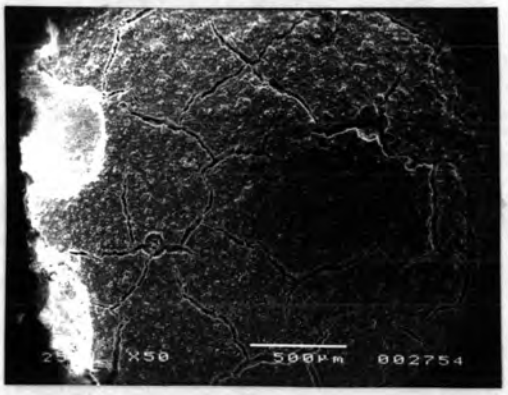

50:50

75:25

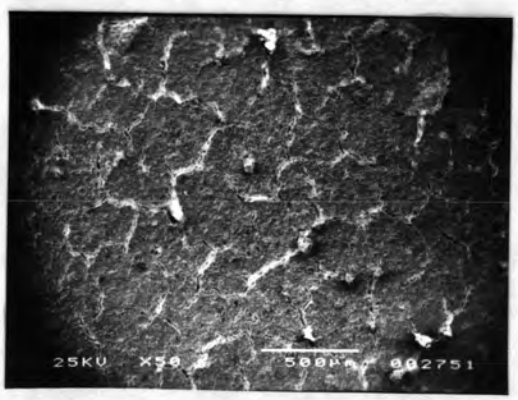

Figure 61-64. Surface condition of coated MP bars sintered at 1200 ^{o}C.

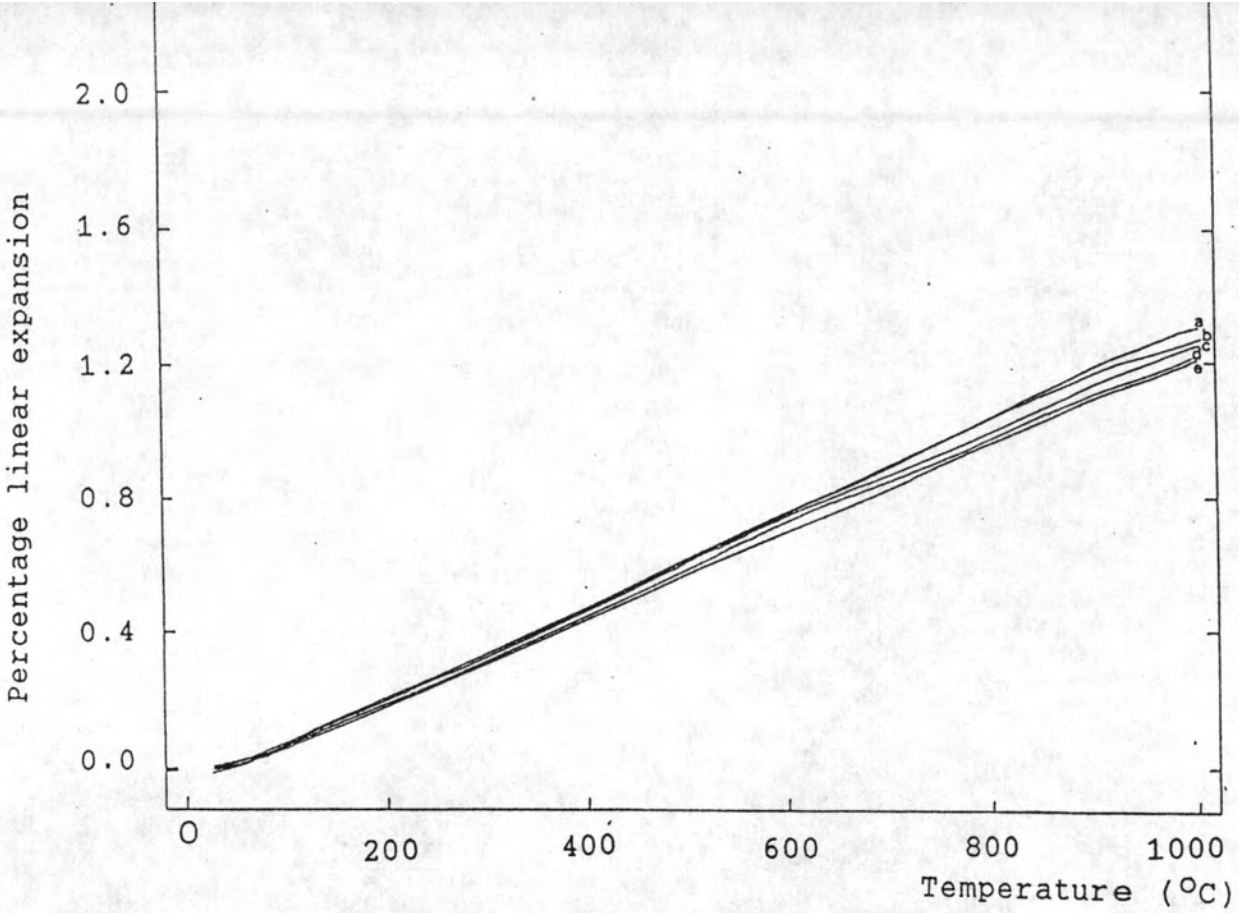

Figure 65. Thermal expansion of various MP:TP compositions sintered at 1200 °C.

MP:TP ratio

a) 0:100

b) 25:75

c) 50:50

d) 75:25

e) 100:0

MP:TP ratio	Thermal expansion cofficient (at 30-1000 °C) $x10^{-6}$ C^{-1}
0:100	13.564
25:75	13.227
50:50	12.936
75:25	12.547
100:0	12.459

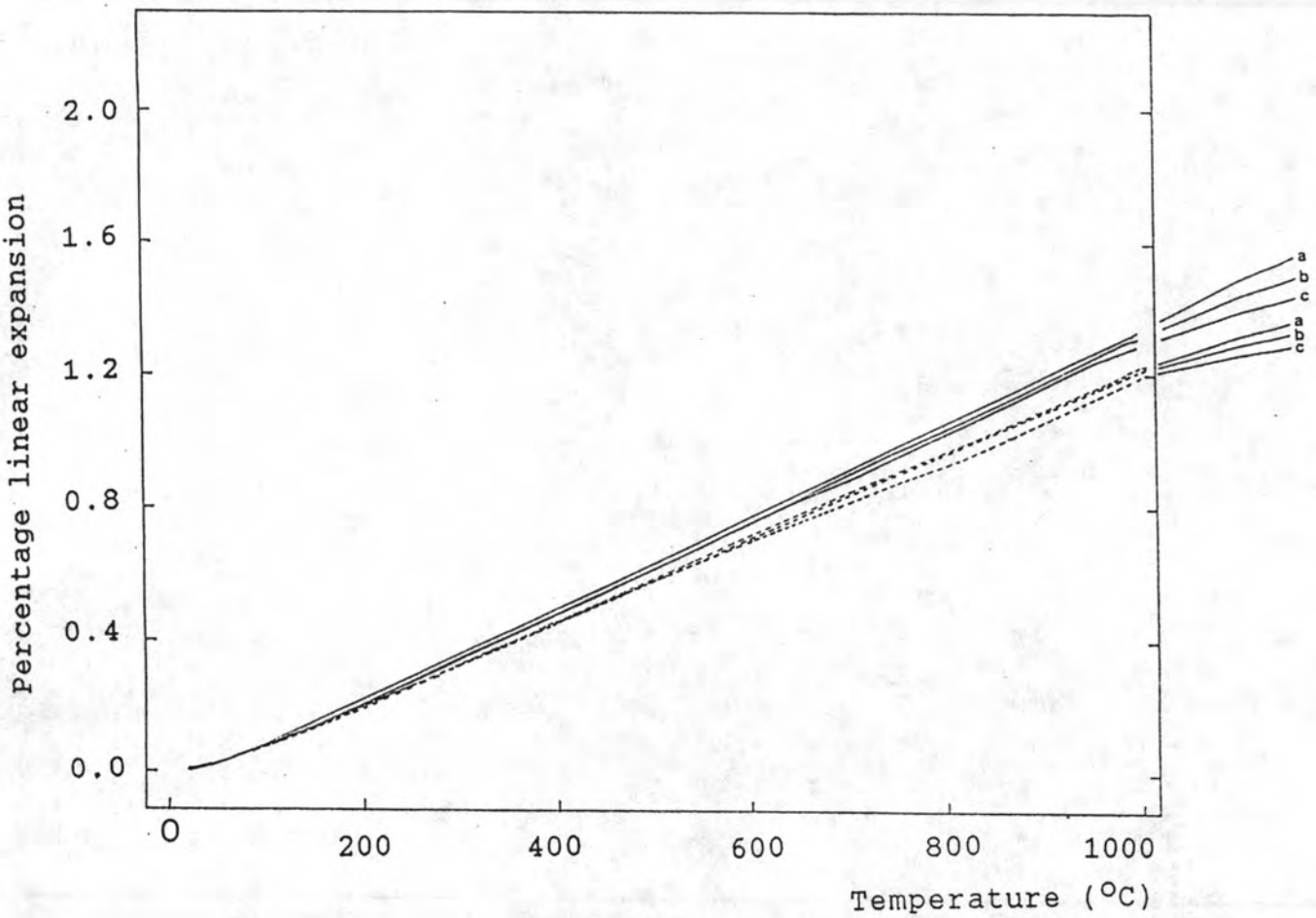

Figure 66. Thermal expansion of MP and TP sintered at various temperatures for 1 h.

a = 1300 °C ———— TP

b = 1200 °C – – – – – – MP

c = 1100 °C

Sintering temperature (°C)	Thermal expansion coefficient (at 30-100 °C) $x10^{-6}$ C^{-1}	
	MP	TP
1100	12.389	13.266
1200	12.459	13.564
1300	12.722	13.792

Surface condition of MP coated with the MP:TP composition = 25:75 and sintered at various temperature was shown in Fig.67-69. The crazing features appeared to be similar. More slightly serious crazing at higher sintering temperature (1300 ^{o}C) might cause by sintering of TP with higher shrinkage that allow continuation of cracking.

1100 ^{o}C

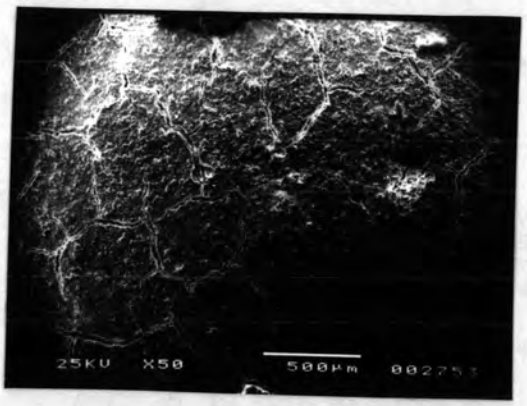

1200 ^{o}C

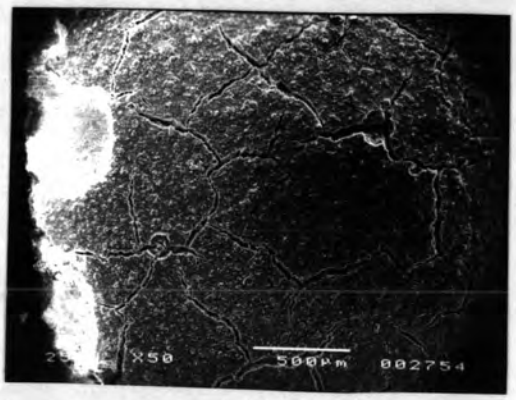

1300 ^{o}C

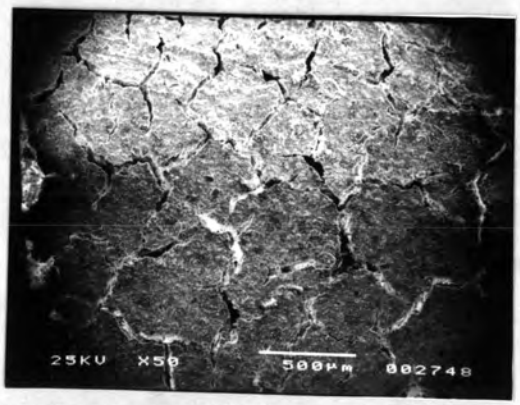

Figure 67-69. Surface condition of MP bars coated with 25:75(MP:TP) coating composition, sintered at 1100, 1200 and 1300 ^{o}C.

4.7.2 TP bars coated with various coating compositions

Peeling obviously appeared at all sintering temperature in TP bars coated with 100% MP. This result came from too low thermal expansion of coating (see fig. 65).

Surface condition of TP bars coated with other coating composition seemed to be smooth (fig.71).

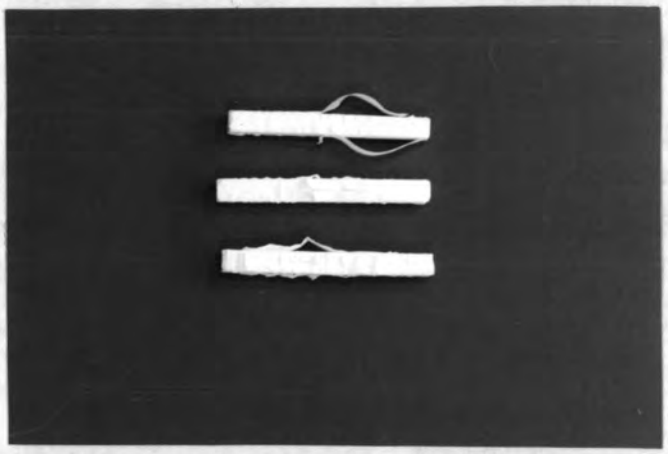

Figure 70. Peeling in TP bars coated with 100% MP.

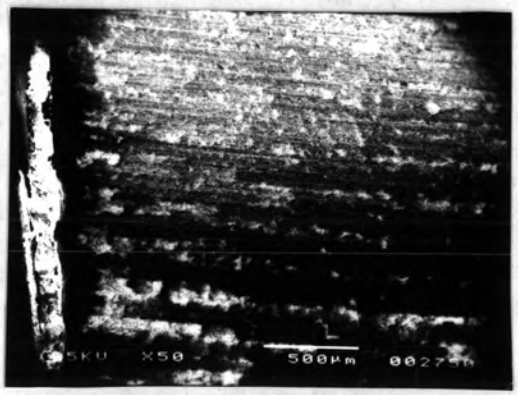

Figure 71. Surface condition of TP bars (MP:TP coating compsition = 75:25)

4.8 Strength of the Products

4.8.1 Flexural Strength of MP Bars

From Fig.72-74, the results showed lower flexural strength of coated MP bars compared with uncoated MP. The strength tended to decrease when TP content in coating composition increased. The declination of strength might come from cracked surface. Flexural strength of all compositions increased with the sintering temperature.

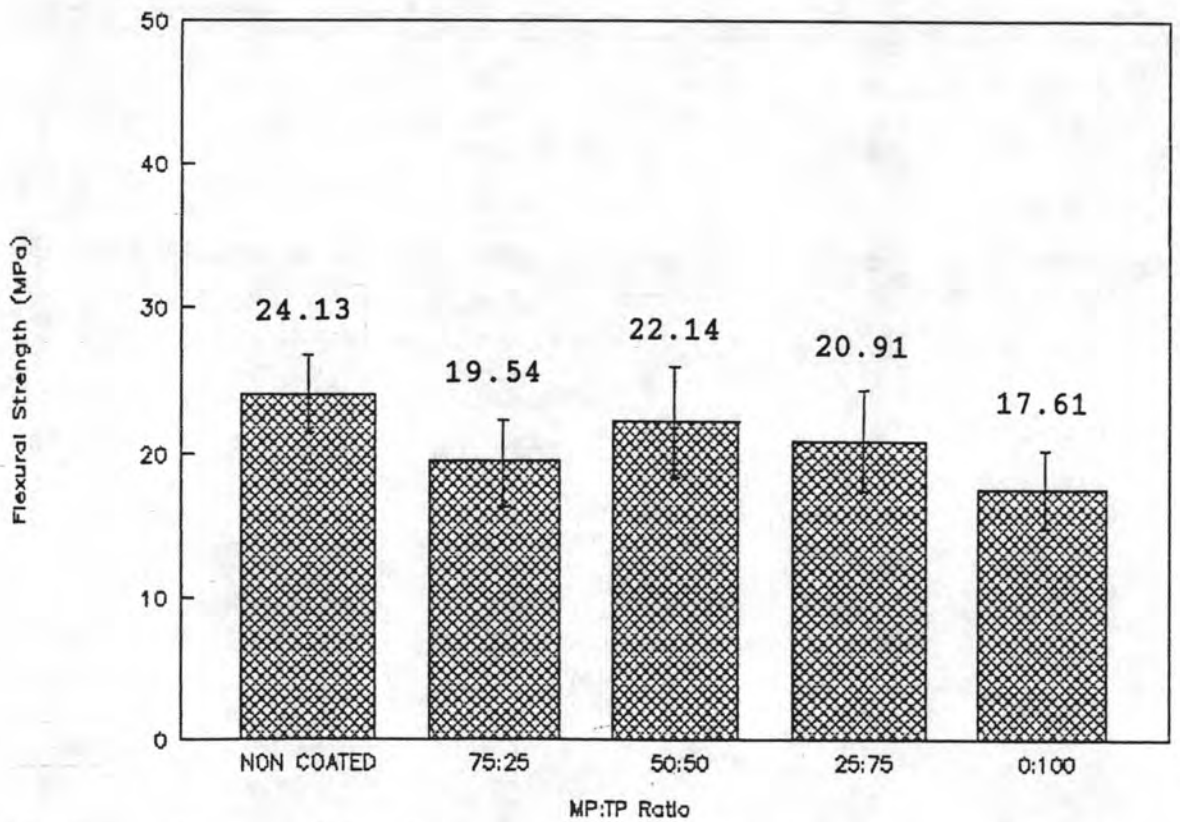

Figure 72. Flexural strength of sintered MP bars, 1100 ^{o}C.

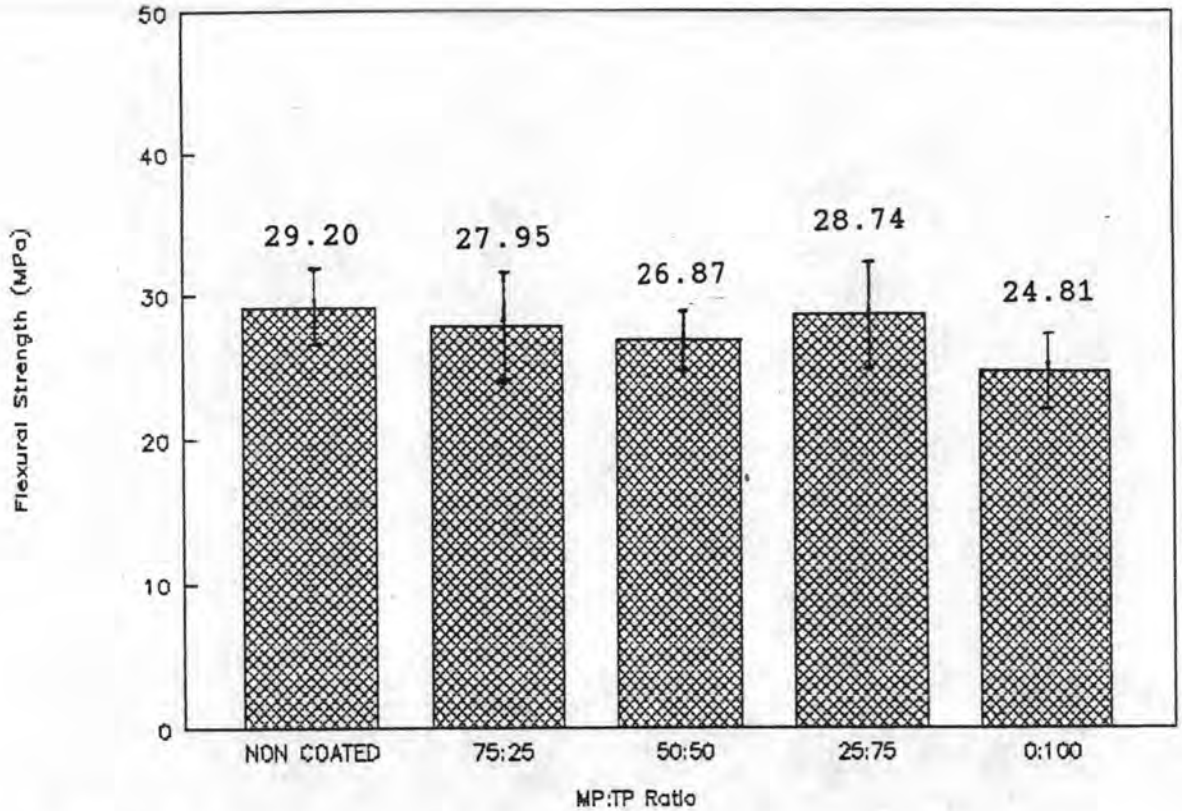

Figure 73. Flexural strength of sintered MP bars, 1200 °C.

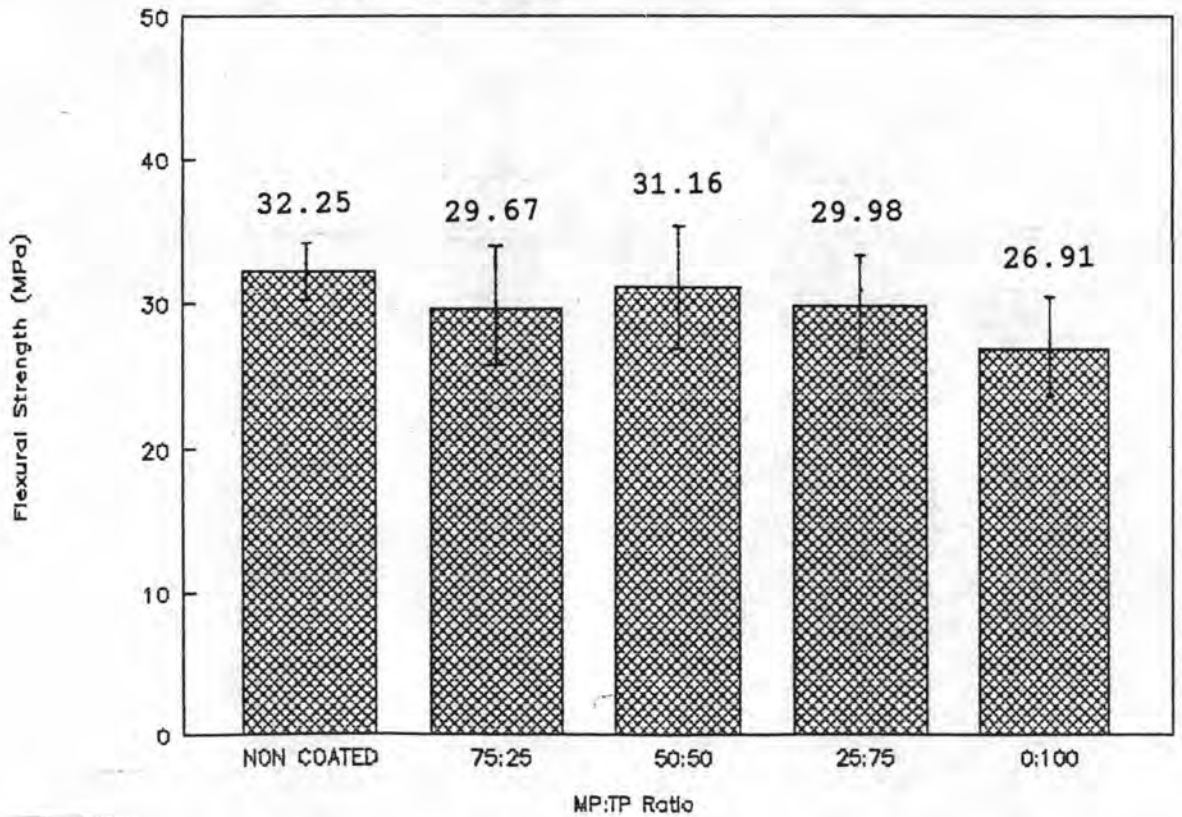

Figure 74. Flexural strength of sintered MP bars, 1300 °C.

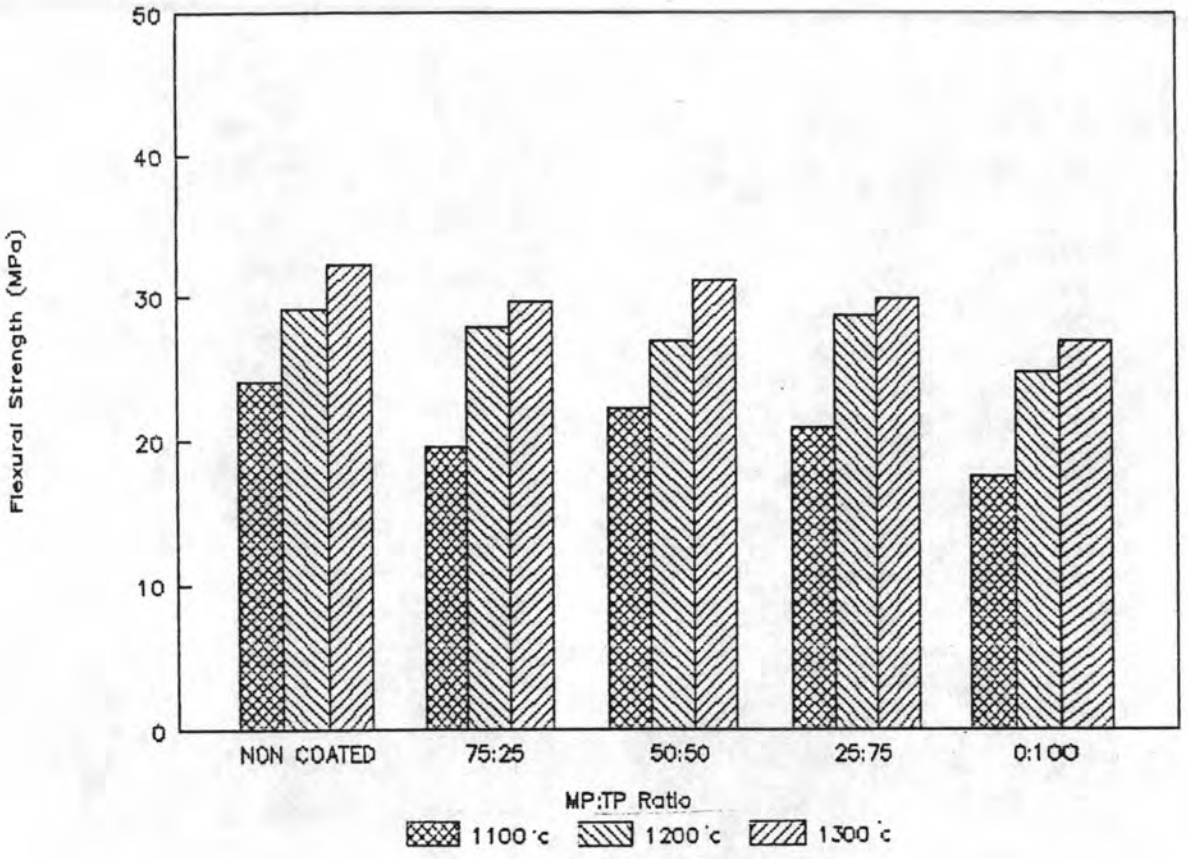

Figure 75. Flexural strength of sintered MP bars.

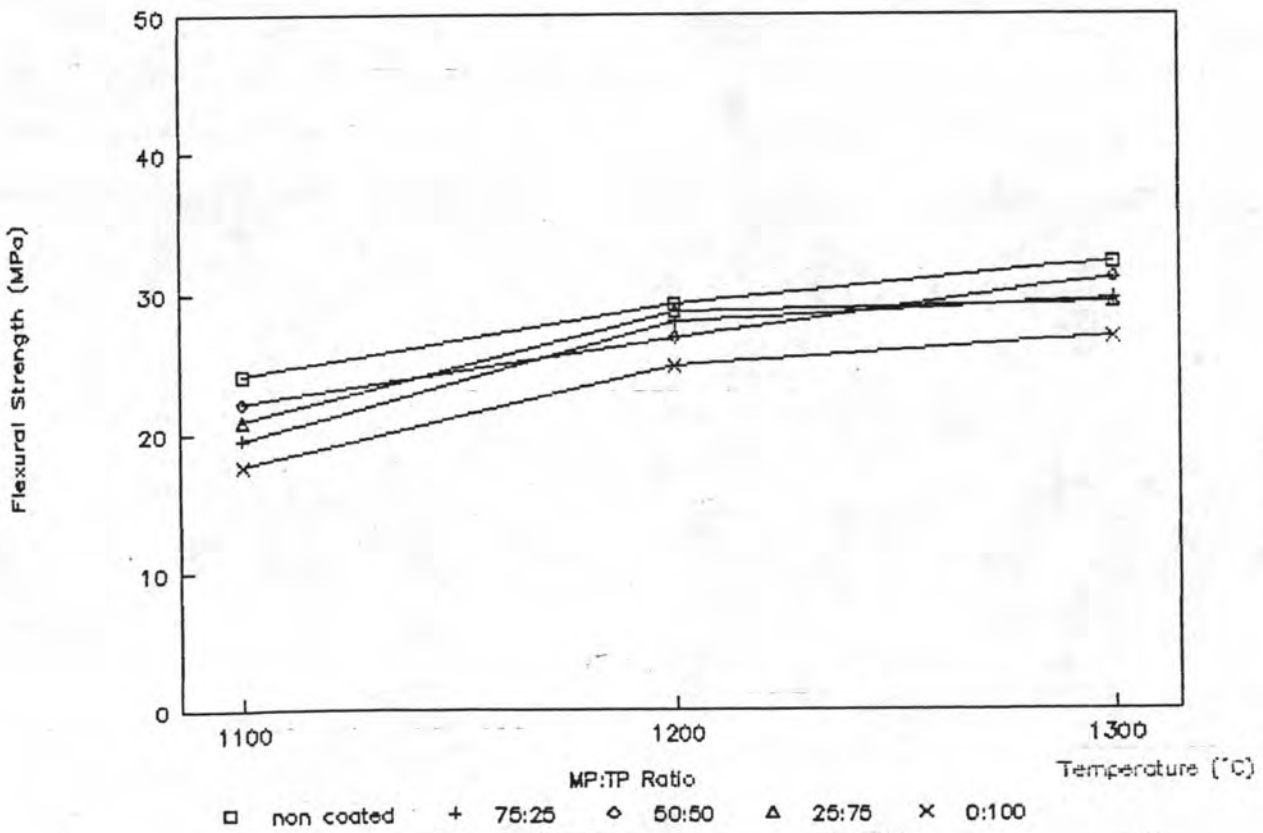

Figure 76. Flexural strength of sintered MP bars.

4.8.2 Flexural Strength of TP bars

Flexural strength of uncoated TP bars and TP bars, coated with various coating compositions and sintered at 1100, 1200 and 1300 ^{o}C was summarized in Fig. 77-81. In all compositions, strength increased when sintering temperature increased. The maximum strength was detected in TP bars coated with 50:50 (MP:TP) coating composition. The lower strength in 75:25 (MP:TP) coating composition could be the result that coating layer did not contact with the body. The strength increase about 5.3, 10.5 and 8.7 % (at sintering temperature 1100, 1200 and 1300 ^{o}C, respectively.) was observed in coated TP (50:50 (MP:TP) coating composition), compared with uncoated TP at the same sintering temperature. The strength increased with the sintering temperature.

TP bars coated with 100% MP coating slip could not be tested because all of them were peeling.

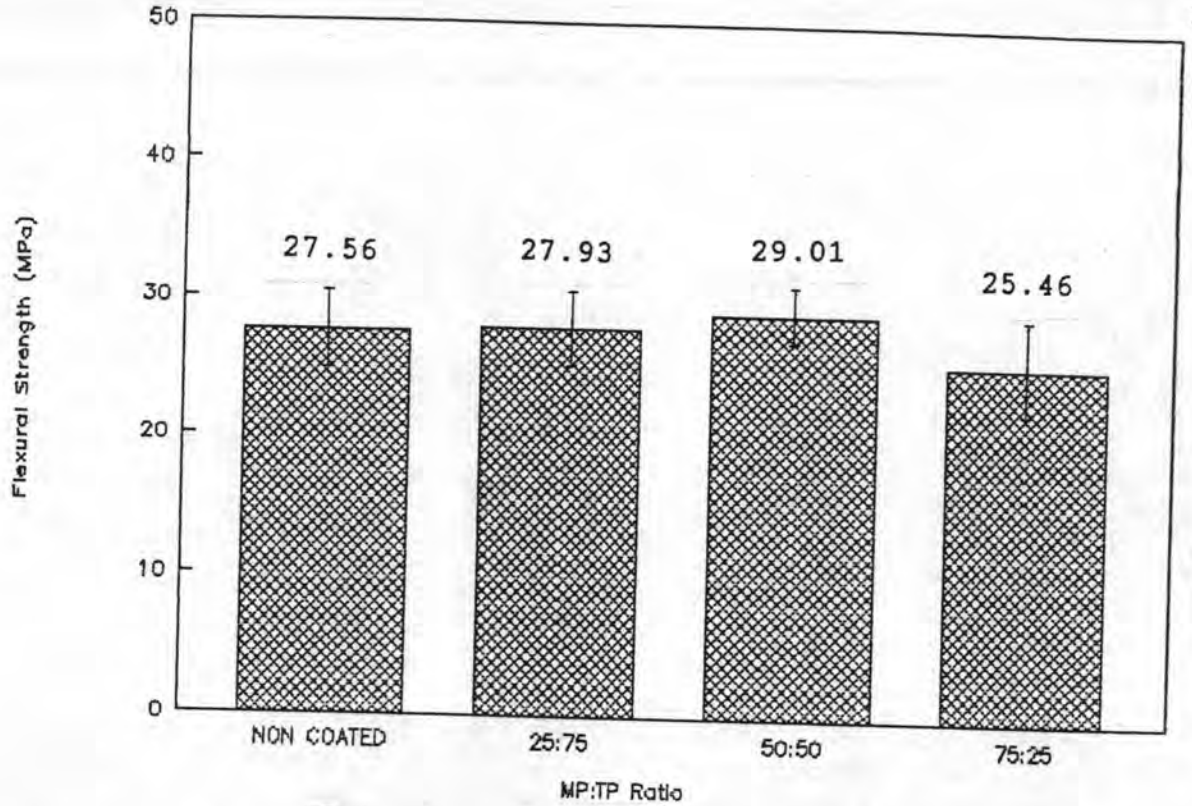

Figure 77. Flexural strength of sintered TP bars, 1100 °C.

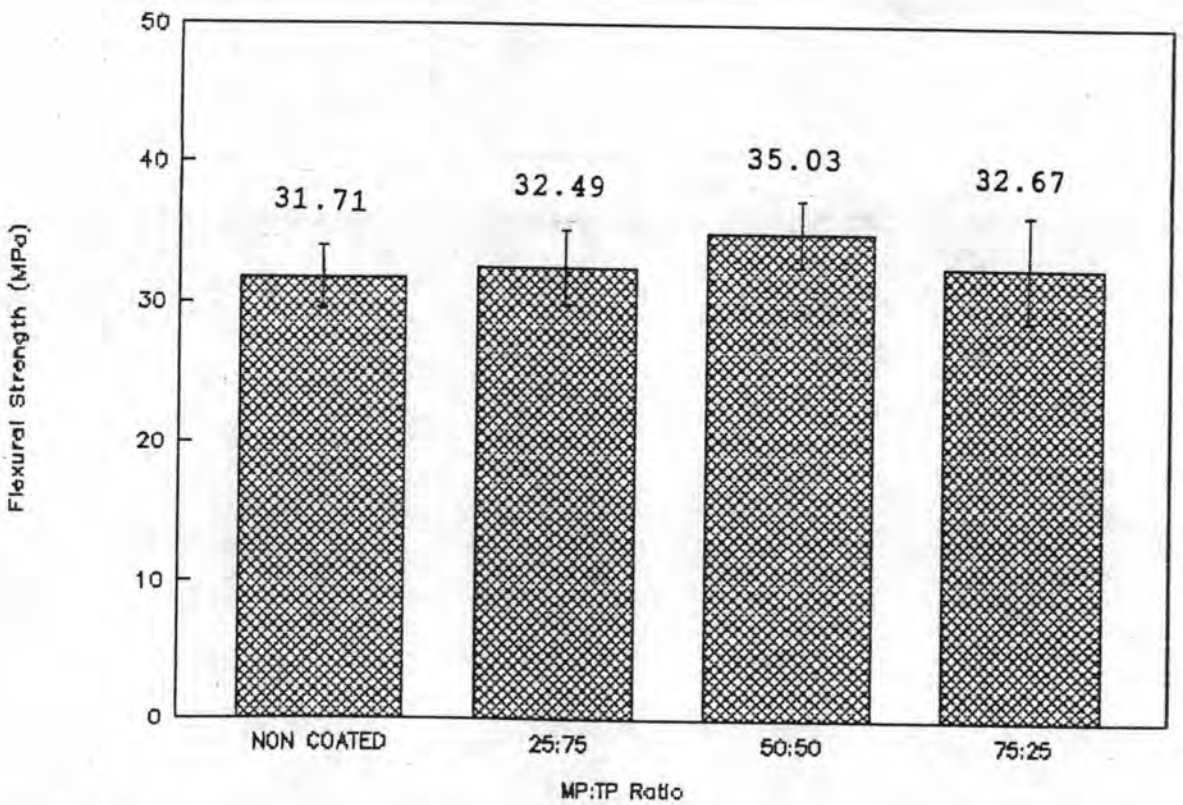

Figure 78. Flexural strength of sintered TP bars, 1200 °C.

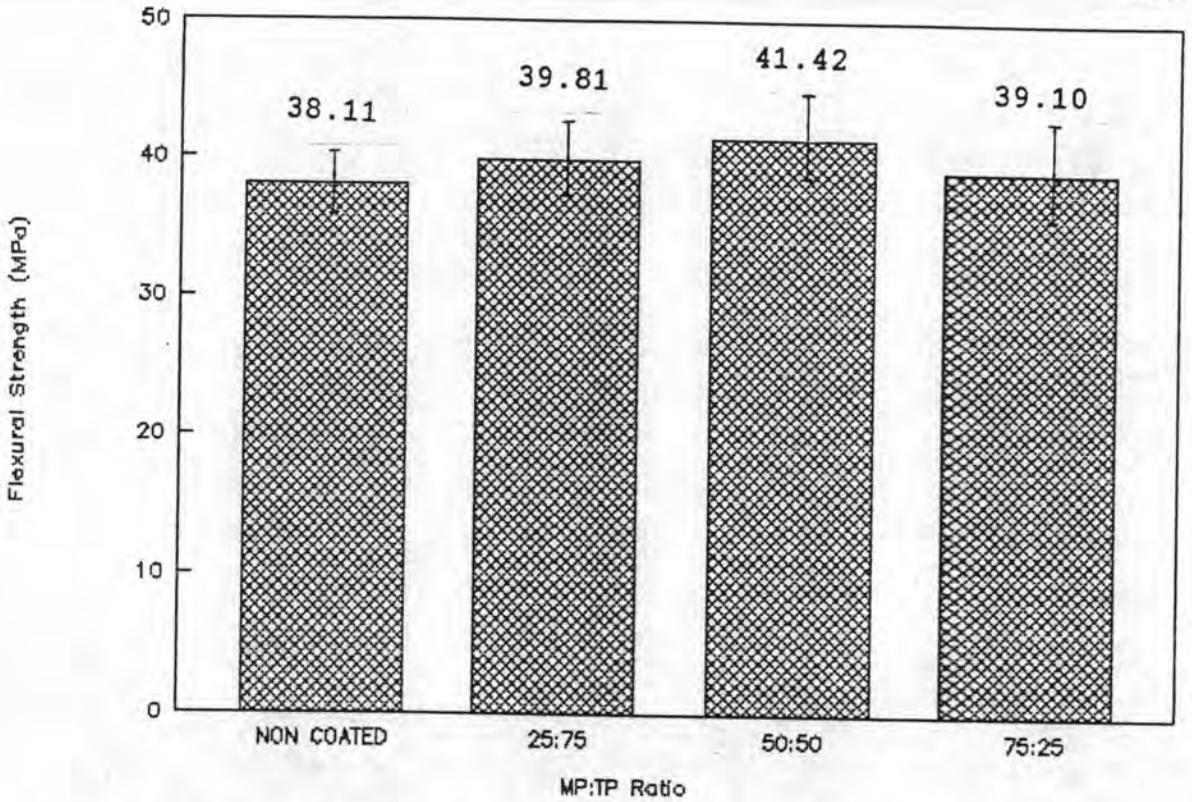

Figure 79. Flexural strength of sintered TP bars, 1300 °C.

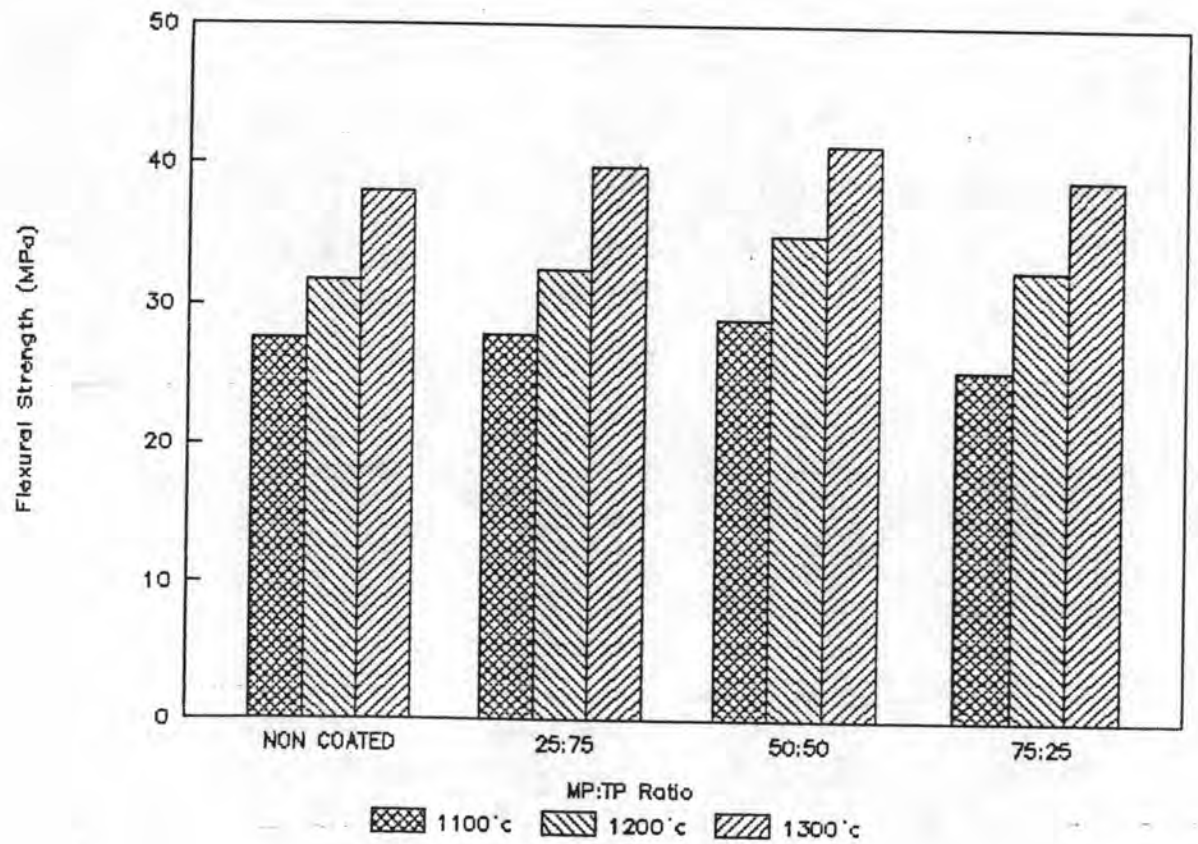

Figure 80. Flexural strength of sintered TP bars.

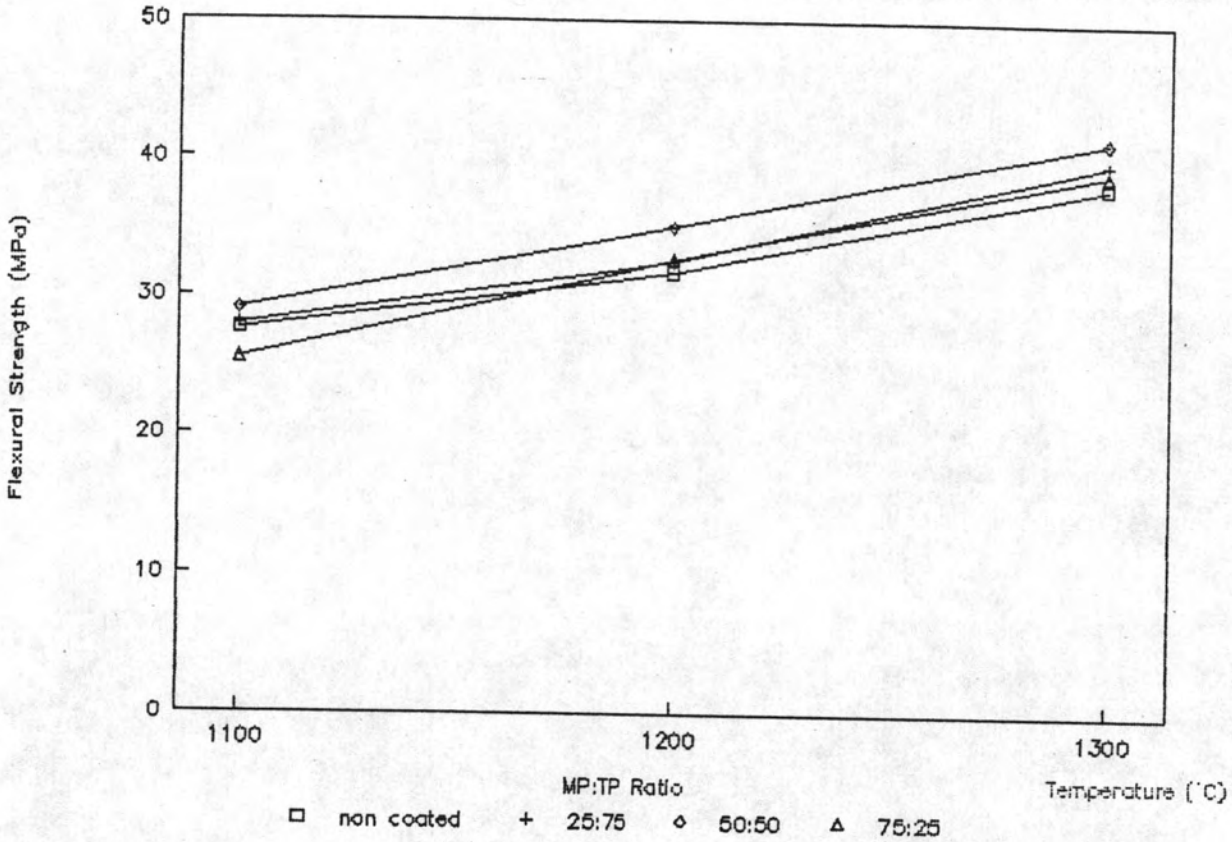

Figure 81. Flexural strength of sintered TP bars.

4.8.3 Compressive Strength

Uncoated MP and TP bars, and coated TP bar which gave maximum strength from flexure testing (50:50 (MP:TP) coating composition), sintered at 1200 ^{o}C, were selected for compressive testing. The strength increase about 4.5 % was observed in coated TP, compared with uncoated TP.

Flexural and compressive strength of all sintered products are summarized in table 11.

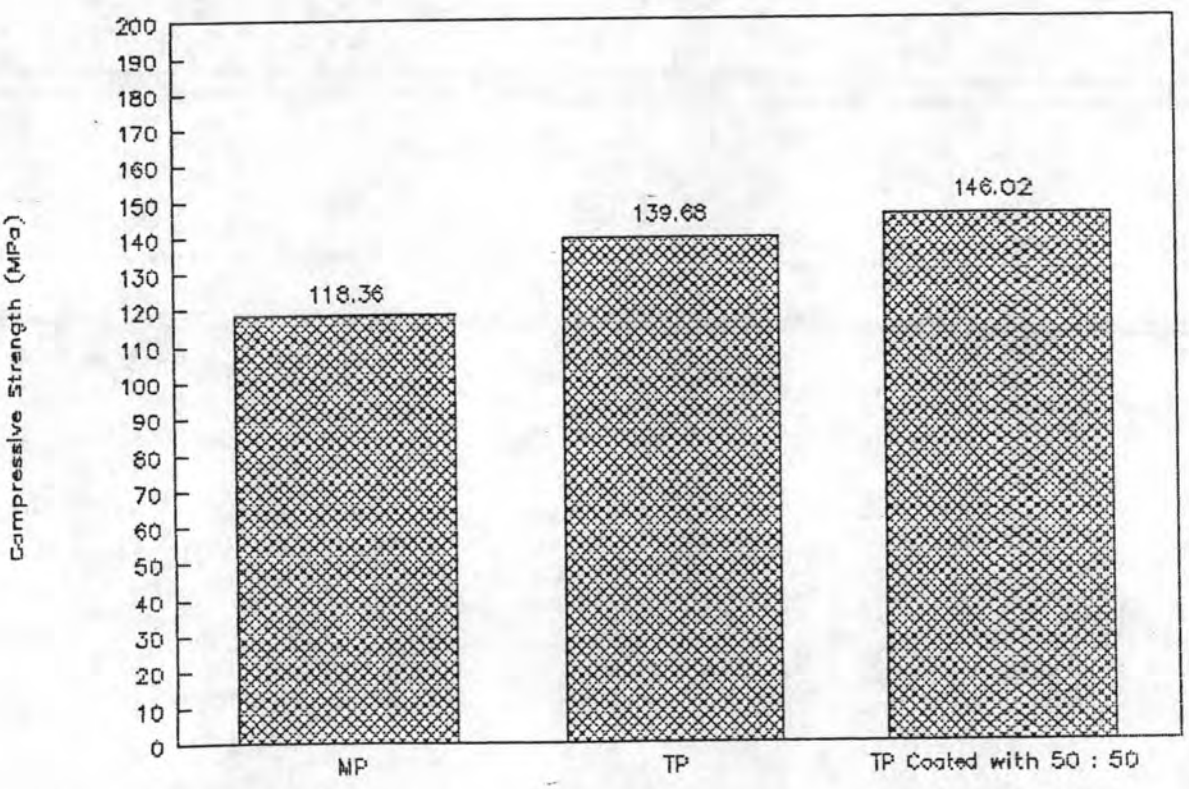

Figure 82. Compressive strength of uncoated MP and TP bars, and TP bars coated with 50:50 (MP:TP) coating composition.
(sintering Temperature 1200 ^{0}C)

body	MP:TP ratio	sintering temp. (°C)	flexural strength (MPa)	S.D.*	compressive strength (MPa)	S.D.
MP	uc#	1100	24.13	2.54		
MP	75:25	1100	19.54	2.94		
MP	50:50	1100	22.14	3.61		
MP	25:75	1100	20.91	3.39		
MP	0:100	1100	17.61	2.64		
MP	uc	1200	29.20	2.61	118.36	32.54
MP	75:25	1200	27.95	3.70		
MP	50:50	1200	26.87	2.21		
MP	25:75	1200	28.74	3.73		
MP	0:100	1200	24.81	2.53		
MP	uc	1300	32.25	1.94		
MP	75:25	1300	29.67	3.81		
MP	50:50	1300	31.16	4.32		
MP	25:75	1300	29.98	3.42		
MP	0:100	1300	26.91	3.36		

(to be continued)

* standard deviation

uncoated

Table 11. Flexural and compressive strength of all sintered products.

continued:

body	MP:TP ratio	sintering temp. (°C)	flexural strength (MPa)	S.D.*	compressive strength (MPa)	S.D.
TP	uc	1100	27.56	2.61		
TP	25:75	1100	27.93	2.59		
TP	50:50	1100	29.01	1.94		
TP	75:25	1100	25.46	3.30		
TP	uc	1200	31.71	2.02	139.68	27.68
TP	25:75	1200	32.49	2.91		
TP	50:50	1200	35.03	2.34	146.02	43.26
TP	75:25	1200	32.67	3.64		
TP	uc	1300	38.11	1.98		
TP	25:75	1300	39.81	2.51		
TP	50:50	1300	41.42	3.12		
TP	75:25	1300	39.10	3.37		

Table 11. Flexural and compressive strength of all sintered products.